International Journal on Science and Technology (IJSAT)
E-ISSN: 2229-7677 ● Website: www.ijsat.org ● Email: editor@ijsat.org

A study on the morning and evening time variation of atmospheric turbulence over Guwahati

Dhrubajyoti Choudhury[1], Dhiman Barua[2],Dhanjit Medhi[3]

[1]Department of Physics, Baosi Banikanta Kakati College Nagaon, Barpeta-781311, Assam, India
[2]Department of Physics, Gauhati University, Guwahati-781014, Assam, India

Abstract:

The process of turbulence generation is always associated with rapid fluctuation of the air density which in turn can modulate the radio refractive index of the atmosphere. Radio waves propagating through such a turbulent medium may undergo severe attenuation. Intensity of the atmospheric turbulence is generally expressed as the refractive index structure constant, generally termed as C_n^2. The knowledge of refractive index structure constant (C_n^2) at different atmospheric regimes is therefore fundamental to determine the impact of turbulence on the signals propagating in the troposphere. Atmospheric turbulence generally regarded as small-scale irregular air motions characterized by winds that vary in speed and direction. In our work, efforts are made to characterize the morning and evening time variation of refractive index structure constant (C_n^2) over Guwahati using radio sonde data. For this work , morning and evening time records of atmospheric sounding for few selected days of 2019 will be utilized to estimate the C_n^2 parameter from surface to the higher altitudes. Further, through this work, the possible mechanisms that may lead to the variations in the vertical turbulence characteristics over this region will also be investigated.

Keywords: Attenuation, Refractive index structure constant, Atmospheric turbulence, Time variation, Radio sonde data, High altitude.

1. Introduction

The process of turbulence generation is always associated with rapid fluctuation of the air density which in turn can modulate the radio refractive index of the atmosphere. Radio waves propagating through such a turbulent medium may undergo severe attenuation. Intensity of the atmospheric turbulence is generally expressed as the refractive index structure constant, generally termed as C_n^2. The knowledge of refractive index structure constant (C_n^2) at different atmospheric regimes is therefore fundamental to determine the impact of turbulence on the signals propagating in the troposphere [1,10,11]. The clear-air radar sensitivity varies proportionally with C_n^2 magnitude [2,13,14]. Sharp inhomogeneities in the atmospheric refractive index can result in the backscatter of the radar power (Bragg phenomenon) [2]. The corrected C_n^2 derivation may improve estimates of the performance of these systems at higher altitude [2]. On the other hand, wind profiling radars, operated vertically at VHF or UHF frequencies are very sensitive to instantaneous variation of radio refractive index. Measurement of atmospheric turbulence at the radar

sites may be very useful for estimating the optimum range that can be attained for a wind profiler. Strength of atmospheric turbulence, estimated in terms of refractive index structure parameter C_n^2 can be expressed as a function of the basic atmospheric variables. The parameter shows a continuous fall in magnitude with height under normal atmospheric condition. But due to the turbulent behaviour of the atmospheric medium at different altitudes, the normal vertical characteristic of C_n^2 is significantly disturbed. At the lower atmospheric regime, the parameter shows unpredictable behaviour which is very much dependent on the seasonal as well as regional features of a particular location [8,9,10,11].

Turbulence plays a very important role in the dynamics of the middle atmosphere by mixing all the atmospheric constituents and also helps them to get distributed both vertically and horizontally [15,16]. Turbulence is characterized by the generation of eddies. Eddies are the packets of turbulent kinetic energy. Larger eddies break in to smaller eddies in a process called energy cascade where some of the inertial energy of the larger eddies is transferred to the smaller eddies [13,14]. This dissipation usually happens only at the smallest size (1 mm diameter) eddies, but it affects all turbulent scales because of the turbulent cascade of energy from larger to smaller scales [16,17]. For turbulence to exist, there must be continual generation of turbulence from shear to buoyancy (usually into the larger scale eddies) to offset the transfer of kinetic energy down the spectrum of ever smaller eddy sizes towards eventual dissipation. The superposition of all scales of eddy motion can be quantified via an energy spectrum, which indicates how much of the total turbulence kinetic energy (TKE) is associated with each eddy scale. It is well known that turbulence in the free atmosphere is confined to thin horizontal layers separated by non-turbulent regions. These layers are limited in horizontal extent and time. This gross turbulence in those layers is, therefore, inherently inhomogeneous, anisotropic and non-steady [19,14]. Whereas, in the interior of the turbulent layers, at scale lengths much smaller than the thickness of the layer, turbulence is observed to be nearly homogeneous and isotropic. Different physical processes are involved with the generation of turbulence in the free atmosphere. At different atmospheric regions, turbulence may be of mechanical or thermal in origins which are driven by different natural processes [11,5]. Mechanical turbulence, also known as forced convection, can form if there is shear in the mean wind field. Such shear can be caused by frictional drag initiated by the topographical orientation of the earth's surface, which causes slower winds near the ground than aloft [12,13,14]. Another factor causing turbulence in the lower atmospheric regime is buoyant convection introduced by the solar heating of the earth's surface. In the middle to upper atmospheric regions, different seasonal and synaptic conditions also generate turbulence [10,16,17].

In this work, efforts are made to characterize the morning and evening time variation of refractive index structure constant, C_n^2 over Guwahati using radio sonde data. For this work, morning and evening time records of atmospheric sounding for few selected days of 2019 will be utilized to estimate the C_n^2 parameter from surface to the higher altitudes. Further, through this work, the possible mechanisms that may lead to the variations in the vertical turbulence characteristics over this region will also be investigated.

2. Data & Methodology

Radio sonde data utilized for this work are obtained from the public domain of the University of Wyoming (http://weather.uwyo.edu/upperair/sounding.html). The data is accessible to the users at an interim of 12 hours. The data set contains information on the atmospheric variables from ground up to high altitudes of

approximately 30 km based on the season and the weather conditions. Each data file contains the instantaneous values of different atmospheric variables as listed below,

1. Atmospheric Pressure in hPa
2. Temperature in degree celsius
3. Wind speed in knot
4. Wind direction in degrees
5. Potential temperature in kelvin
6. Equivalent Potential temperature in kelvin
7. Virtual Potential temperature in kelvin
8. Relative humidity in %
9. Relative humidity with respect to ice in %
10. Dewpoint Temperature in Celsius
11. Frost Point Temperature in Celsius
12. Mixing ratio in g/kg

For our study we selected Guwahati station (lat: 26.2N , lon: 91.75E) and the necessary atmospheric information are extracted as per requirement. All the data fields in the daily radio sonde files are recorded at some non-uniform atmospheric levels. To study the time variation of a parameter at different atmospheric layers, all the data points should be made available at some common/standard levels of the atmosphere. Therefore, each data fields are interpolated to some standard atmospheric levels for our analysis.

A single atmospheric sounding is sufficient to draw the vertical distribution of the basic atmospheric variables and the associated atmospheric parameters. As representative plots, temperature, pressure, humidity, zonal wind(u), meridional wind(v) and log(C_n^2) for both 00z and 12z of 11 January 2019are presented in figure (1).

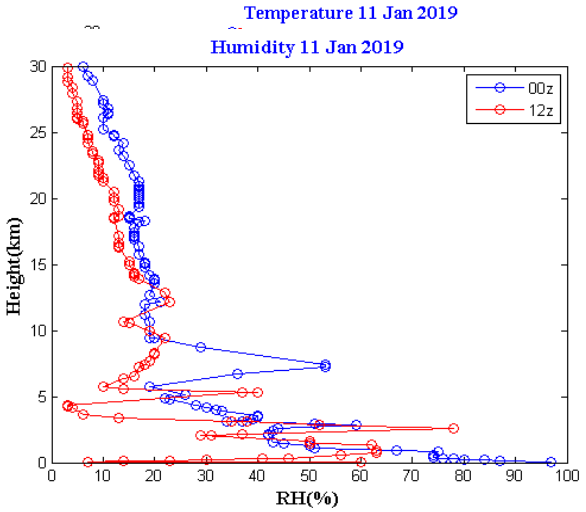

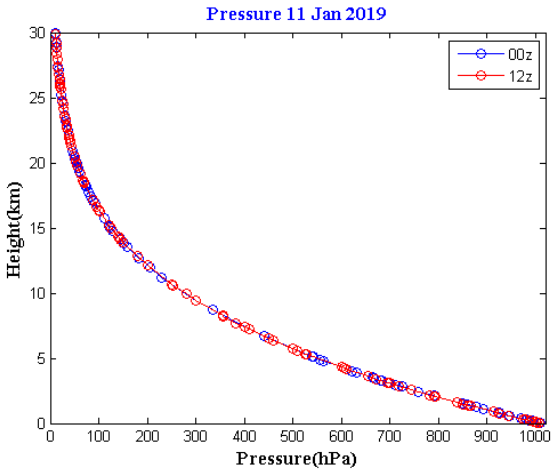

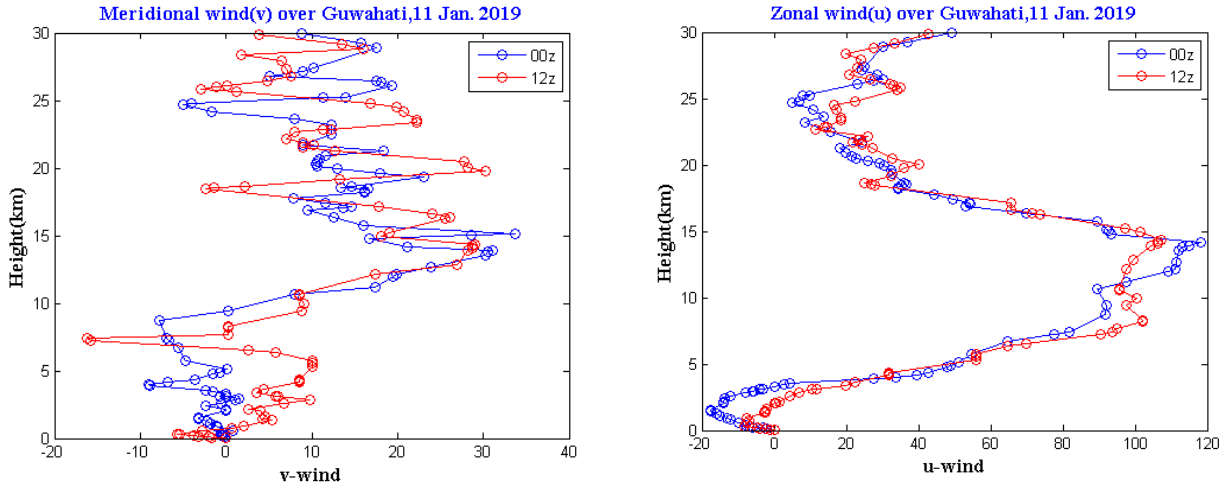

Figure 2.1: Vertical distribution of temperature, pressure, humidity, u wind and v wind over Guwahati on 11.01.2019

It is observed from the above distributions that, temperature in the morning hour is relatively low as compared to the afternoon record close to the ground. But at upper levels of the atmosphere the differences are not significant between the 00z and 12z profiles. Two shallow inversion layers are observed at 200 m and 3.5 km above ground in the 00z profile. Beyond 4 km temperature profiles follow the normal trend up to the tropospheric height. Tropopause heights at both the hours are observed at around 14.8 km. Above tropopause, effect of strong westerly wind is clearly visible on the temperature profiles where a slight decrease of temperature is seen. Pressure profiles for both the sounding show a clean monotonic decrease with altitude. In the morning sounding surface pressure was higher (1010 hPa) as compared to the afternoon surface pressure (1007 hPa). Surface humidity at 00z was higher than the 12z humidity. It may be due to the fact that, during the afternoon hours a well-established convective activity mixes all the atmospheric constituents both vertically and horizontally and hence reduces the humidity concentration in the near earth environment. Due to the absence of significant convective activity during the morning hours, high humidity is seen near the ground. From the plots of u wind it is observed that up to 2.5 km above ground wind is easterly and beyond that westerly components are observed at all the atmospheric levels. If we look at the meridional wind profiles, it is observed that during the 12z hour, southerly wind is significant up to 5km of altitude. Whereas at 00z northerly wind is observed up to 5 km. Beyond 9 km of altitude southerly wind prevails up to the tropospheric height.

3. Estimation of Turbulence Structure Constant Parameter (C_n^2)

The structure function of the velocity field in the inertial subrange satisfies a universal 2/3 power law [2]. The turbulent fluctuations of the atmospheric refractive index 'n' along the distance 'r' are described by the refractive index structure function $D_n(r)$ [2]. For locally isotropic turbulence fields, the structure function of the velocity field can be expressed as

$$D_n(r) = \langle [n(x)-n(x+r)]^2 \rangle = C_n^2 r^{2/3}$$

where C_n^2 is the refractive index structure coefficient and can be considered to be a measure of the

strength of small scale turbulence. Here, angle brackets define the spatial average [2].

In homogeneous isotropic turbulence, the turbulence structure constant for the radio-refractivity is given by

$$C_n^2 = \alpha^2 \alpha' l_0^{\frac{4}{3}} M^2 \qquad (3.1)$$

where α^2 is a constant = 2.8, α′ the ratio of eddy diffusivities ~ 1, l_0 the buoyancy/outer scale length of the turbulence spectrum and M is the vertical gradient of the potential refractive-index fluctuations. The total turbulent energy density spectrum consists of the production region, the inertial subrange and the dissipation region. Most of the turbulent energy production occurs at scale sizes between $6l_0$ and $l_0/6$, where lo is defined as the generic buoyancy/outer scale of turbulence and $l_0/6$ is defined as the onset of inertial sub-range. In this study, the turbulent scale length (l_0) is considered to be 10 m [3]. The value of M is given by the relation,

$$M = -77.6 \times 10^{-6} \times \left(\frac{P}{T}\right) \times \left(\frac{\partial ln\theta_T}{\partial z}\right) \times \left[1 + \frac{15500q}{T}\left(1 - \frac{1}{2}\frac{\frac{\partial lnq}{\partial z}}{\partial ln\theta_T/\partial z}\right)\right] \ldots\ldots (3.2)$$

where P is the atmospheric pressure (mb), T is the absolute temperature (K), θT is the potential temperature (K), q is the specific humidity (g/kg) and z is the altitude (m) [3].

Again, to calculate the value of specific humidity (q), the following equations are used :

$$ew = 6.1078 \times exp\{17.2694 \times \left(\frac{temp.in\ C}{temp.in\ C+237}\right)\} \ldots\ldots (3.3)$$

$$e = \left(\frac{(Rel.Humi.\ in\ \%) \times ew}{100}\right) \ldots\ldots (3.4)$$

$$q = \frac{0.662 \times e}{(P - 0.378 \times e)} \left(\frac{kg}{kg}\right) \ldots\ldots (3.5)$$

The above equations (1), (2), (3), (4) & (5) are used to calculate C_n^2. A representative plot of $\log(C_n^2)$ is presented in Figure(3.1). Vertical $\log(C_n^2)$ distributions at 00z and 12z shows similar trend from ground up to the upper atmosphere. For both the soundings, structure constant values are high at near earth environment and the magnitudes of C_n^2 decreases with increasing altitudes. During the afternoon hours C_n^2 values are higher at lower levels of the atmosphere as compared to the morning hours.

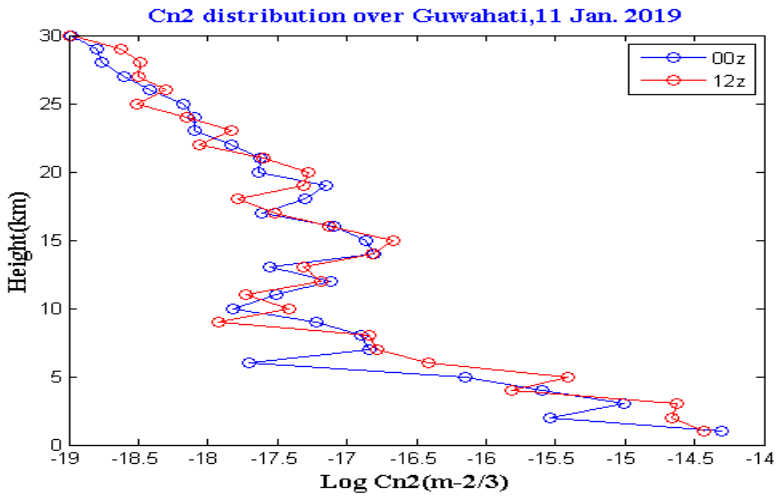

Figure 3.1: Vertical distribution of log(C_n^2) on 11.01.2019 over Guwahati at 00z and 12z.

4. Analysis & Result

To study the turbulence characteristics of the atmosphere over Guwahati, 12 days are randomly selected from each month of 2019 (**Table 4.1**). Morning and evening time atmospheric information are collected for the selected days and data conditioning is performed by re-arranging the vertical data into common atmospheric levels. Then the vertical gradients of temperature, potential temperature and specific humidity are estimated up to a height of 30 km above the ground level. Utilizing the above parameters, vertical gradient of the potential refractive index is calculated for each level of the free atmosphere. Finally, C_n^2 values for all those cases are evaluated using equation (1). Vertical distribution of the logarithm of the refractive index structure constant for the 12 representative days of 2019 are presented in figure 3. Corresponding humidity and the wind speed plots for all the selected cases are also presented in figure (4) and (5). Log(C_n^2) distribution for 00z and for 12z are represented by blue and red lines respectively. From all the cases, 00z hour log (C_n^2) values vary between -13.8 at the lowest level and -19.2 at 30 km. The same variation during the 12z is observed to be between 13.4 to 19.1. Maximum, minimum and standard deviation of log(C_n^2) at all the atmospheric levels for all the cases are summarized in table 2. It is observed from the log(C_n^2) profiles that, log (C_n^2) magnitude vary between -19.03 to -14.29 during 00z while the same variation for 12z is -19.15 to -14.32 during 27th January,2019.

During the afternoon, high values of structure constant is seen at lower heights as compared to the morning time profile. This variability may be the result of the atmospheric convective activity. The same variation on 18th February was observed to be -18.97 to -14.95 during 00z and -19.05 to -14.90 for 12z. At high altitude, just below the tropopause spikes are observed at both 00z and 12z of the C_n^2 profiles of 18th February. These spikes may be the result of high wind shear gradient at those levels. In case of March

Table 4.1

Case No	Date	Morning sounding (00z hrs)		Evening sounding (12z hrs)	
		Min height(m)	Max height(m)	Min height(m)	Max height(m)
1	27.01.2019	54	34216	54	33814
2	18.02.2019	54	31027	54	33268
3	20.03.2019	54	32454	54	31637
4	23.04.2019	54	31728	54	31080
5	22.05.2019	54	33495	54	32021
6	08.06.2019	54	32899	54	32876
7	17.07.2019	54	28135	54	31290
8	18.08.2019	54	31694	54	27144
9	19.09.2019	54	32467	54	33611
10	19.10.2019	54	17935	54	34476
11	12.11.2019	54	33341	54	30910
12	03.12.2019	54	33412	54	33986

month case, log (C_n^2) values vary between -19.07 to -14.50 for 00z and from -18.86 to -14.74 for 12z. In the morning profile, an abrupt rise in structure constant vale is observed at 5km altitude. This enhancement may be the result of instantaneous rise in humidity content at that level which is also confirmed by the

Table 4.2

MONTH	00Z			12Z		
	MAX	MIN	SD	MAX	MIN	SD
JAN	-14.2911	-19.0314	1.138634	-14.3241	-19.1544	1.173244
FEB	-14.958	-18.972	1.167121	-14.9025	-19.0577	1.133758
MAR	-14.5064	-19.0722	1.220908	-14.7402	-18.8633	1.167826
APR	-14.207	-18.9668	1.273693	-14.2521	-19.3728	1.311198

MAY	-14.3819	-19.0624	1.246097	-14.2262	-18.9686	1.380889
JUN	-14.8939	-19.0064	1.250771	-14.3053	-18.9606	1.463324
JUL	-14.1397	-18.6566	1.320611	-14.4651	-19.0472	1.28144
AUG	-14.4466	-19.0618	1.335763	-14.8324	-18.614	1.203276
SEP	-14.1232	-19.2168	1.380819	-13.6954	-19.1949	1.418108
OCT	-13.9025	-18.2366	1.293395	-13.4953	-19.046	1.495443
NOV	-14.1972	-18.9965	1.244951	-14.1666	-19.2203	1.242643
DEC	-14.5768	-19.0645	1.01253	-14.1395	-19.1094	1.206581

humidity distribution at 5km of 20 March 2019. On 23rd of April, variations in the log (C_n^2) values are observed between -18.96 to -14.20 for 00z and from -19.37 to -14.25 during 12z. At an altitude of 8km above ground, a fall in turbulence strength is seen in the evening profile. This may be correlated to the negative gradient in humidity characteristics at that height. On 22nd May, log (C_n^2) values vary from -19.06 to -14.38 at 00z and -19.30 to -13.38 at 12z and the evening time structure constant minimum is lower by an order than the morning time minimum. In June 8, log (C_n^2) values vary from -19.00 to -14.89 during 00z while the same variation at 12z was -18.96 to -14.30. Between 15 and 20 km, an increase of C_n^2 is observed which is almost same both during morning and afternoon time. The humidity profile of 8th June also shows a sharp rise in moisture content at high altitude. Therefore the abrupt enhancement in the C_n^2 profile may be the result of high moisture gradient at those levels. On 17th July, log (C_n^2) values vary between -18.65 to -14.13 during 00z and -19.04 to -14.46 at 12z. In the morning time profile of the July case, maximum C_n^2 magnitude is observed at 5km altitude. A rapid fluctuation in the moisture content can also be seen in the humidity profile of the 00z at around 5 km height which may be the factor responsible for the peak in the C_n^2 profile. The log (C_n^2) variation in 18 August was from -19.06 to -14.44 at 00z and from -18.61 to -14.83 at 12z. Peaks are observed in the log(C_n^2) profiles of both morning and evening between 5-10 km and 15-20 km where humidity profiles also show significant variabilities.

In the profiles of June, July and August, C_n^2 exhibits measurable variations in the upper level. This may the result of sufficient supply of moisture by the monsoon wind at those levels of the atmosphere. log (C_n^2) values vary between -19.21 to -11.93 at 00z and from -19.19 to -13.69 for 12z during 19th September,2019. The same variation in 19 October was from -18.23 to -13.90 and -19.04 to -13.49 at 00z and 12z respectively. In both the months, sharp increase of turbulent strength was observed above the tropopause level. From the November month cases, lowest C_n^2 value observed was 14.16 at 12z and the corresponding maximum was -19.22. The same trend was also observed in the case of 3rd December where the minimum structure constant value was -14.13 at 12z. It is observed from the above that, average structure constant values are higher at the lower atmospheric levels as compared to the high altitude values.

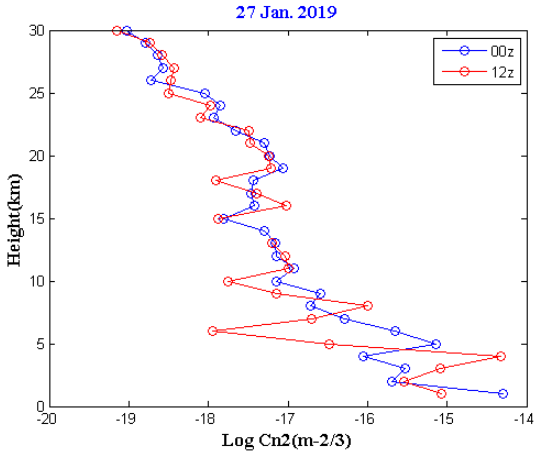
27 Jan. 2019
00z
12z
Height(km)
Log Cn2(m-2/3)

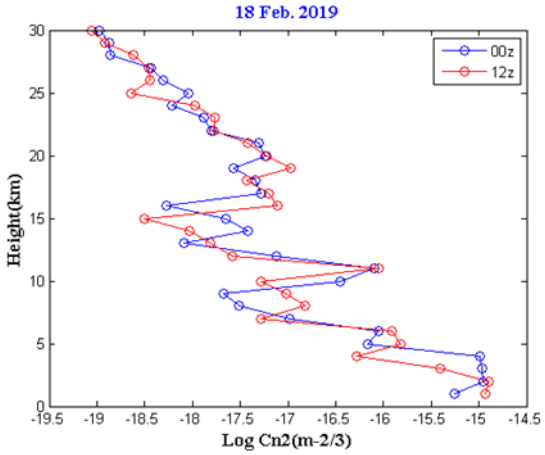
18 Feb. 2019
00z
12z
Height(km)
Log Cn2(m-2/3)

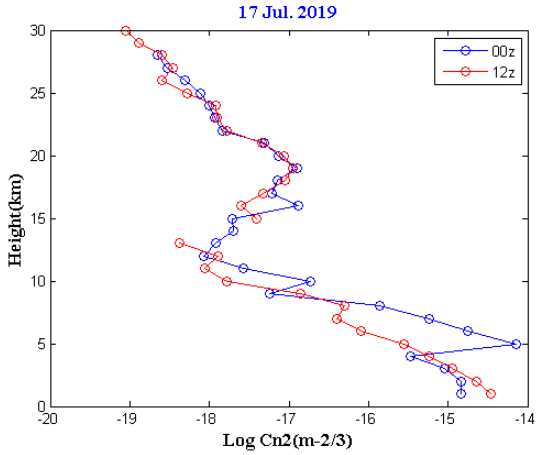
17 Jul. 2019
00z
12z
Height(km)
Log Cn2(m-2/3)

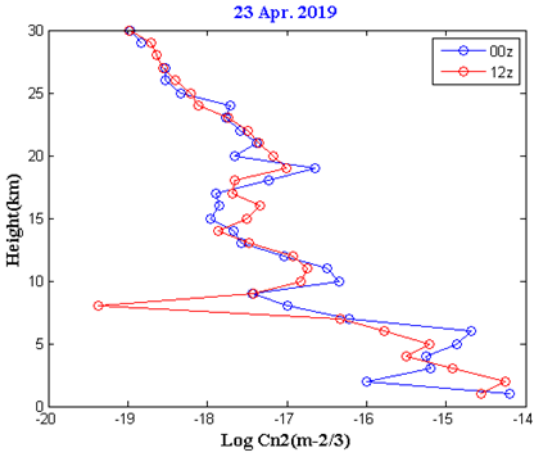
23 Apr. 2019
00z
12z
Height(km)
Log Cn2(m-2/3)

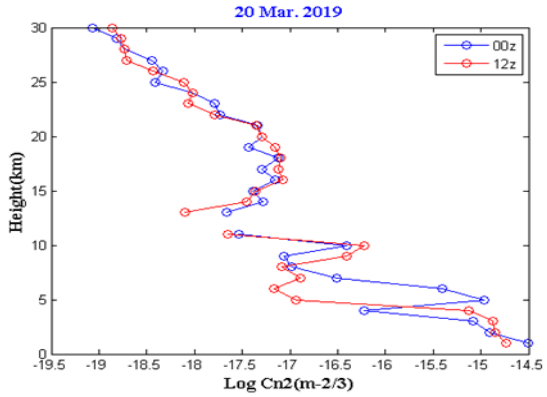
20 Mar. 2019
00z
12z
Height(km)
Log Cn2(m-2/3)

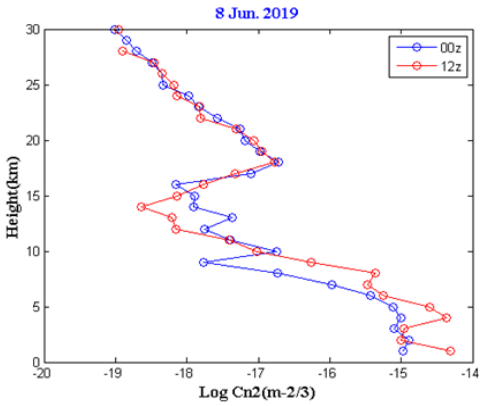
8 Jun. 2019
00z
12z
Height(km)
Log Cn2(m-2/3)

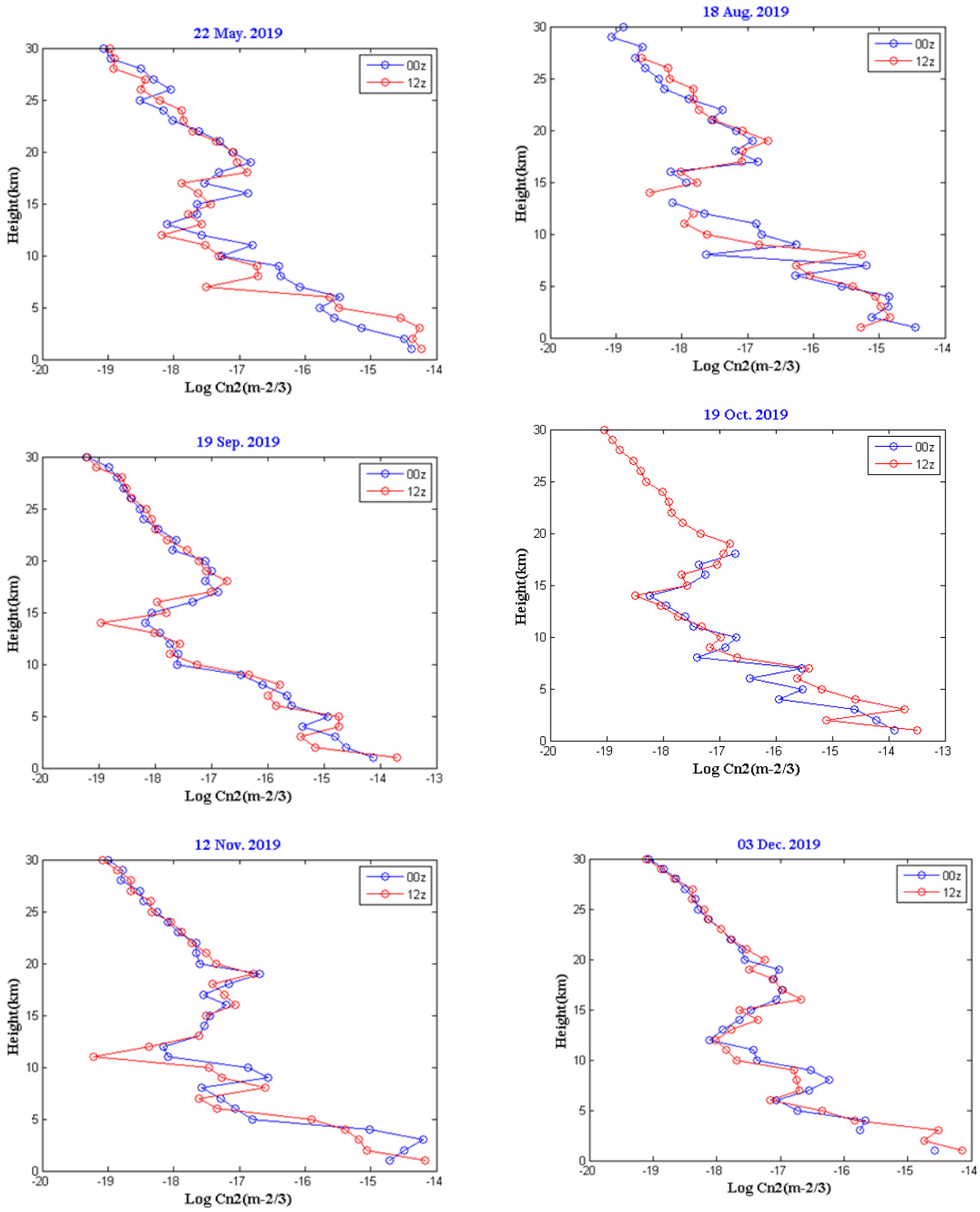

Figure 4.1: Vertical distribution of log(C_n^2) during 00z and 12z for the selected days.

The reason behind this may be the higher moisture and temperature gradient that generally exists at lower atmospheric levels. It is also confirmed from the humidity profiles that, humidity magnitude is very high up to the boundary layer in all the season. It is also seen that, at the higher atmospheric levels variations of moisture content during 00z and 12z is very less for all the cases except the monsoon months. During the monsoon period, the south-west wind pattern adds substantial moisture to the upper atmospheric levels.

Lower atmosphere also experiences all sort of natural and surface process. Among those the orographic and thermal processes are the primary sources that can directly modulate the near surface environment. And therefore, unpredictable fluctuations in the profiles of all the parameters are always seen at lower atmospheric levels.

Table 4.3

MONTH	00Z			12Z		
	MAX	MIN	SD	MAX	MIN	SD
JAN	-14.2911	-19.0314	1.138634	-14.3241	-19.1544	1.173244
FEB	-14.958	-18.972	1.167121	-14.9025	-19.0577	1.133758
MAR	-14.5064	-19.0722	1.220908	-14.7402	-18.8633	1.167826
APR	-14.207	-18.9668	1.273693	-14.2521	-19.3728	1.311198
MAY	-14.3819	-19.0624	1.246097	-14.2262	-18.9686	1.380889
JUN	-14.8939	-19.0064	1.250771	-14.3053	-18.9606	1.463324
JUL	-14.1397	-18.6566	1.320611	-14.4651	-19.0472	1.28144
AUG	-14.4466	-19.0618	1.335763	-14.8324	-18.614	1.203276
SEP	-14.1232	-19.2168	1.380819	-13.6954	-19.1949	1.418108
OCT	-13.9025	-18.2366	1.293395	-13.4953	-19.046	1.495443
NOV	-14.1972	-18.9965	1.244951	-14.1666	-19.2203	1.242643
DEC	-14.5768	-19.0645	1.01253	-14.1395	-19.1094	1.206581

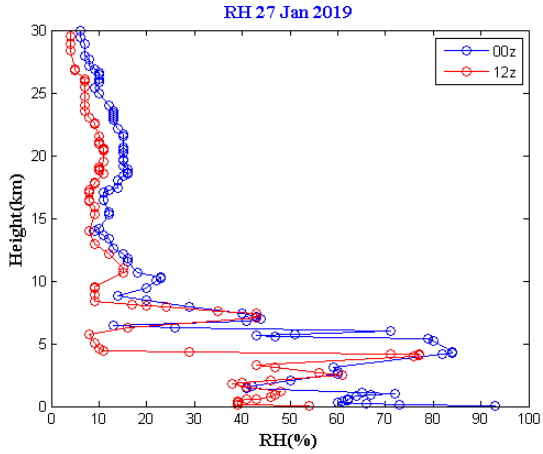
RH 27 Jan 2019
00z
12z
Height(km)
RH(%)

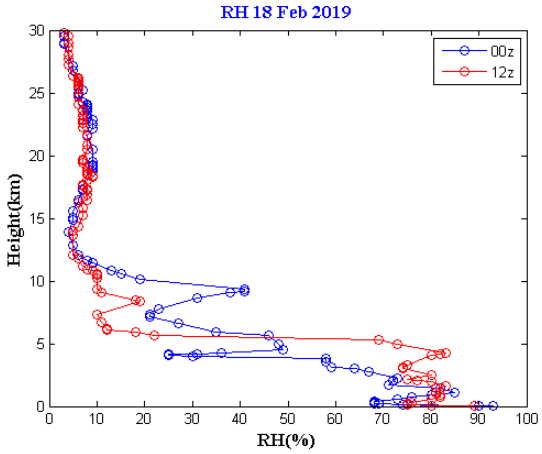
RH 18 Feb 2019
00z
12z
Height(km)
RH(%)

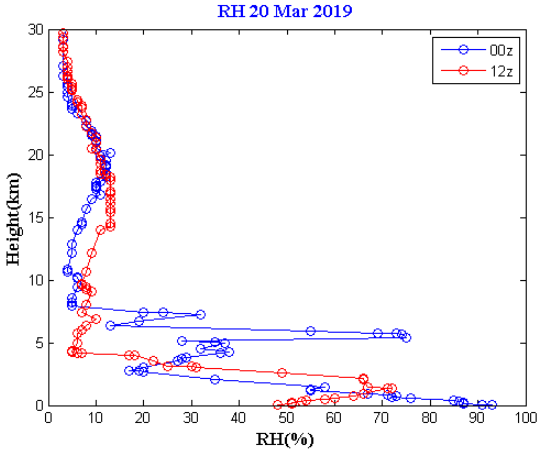
RH 20 Mar 2019
00z
12z
Height(km)
RH(%)

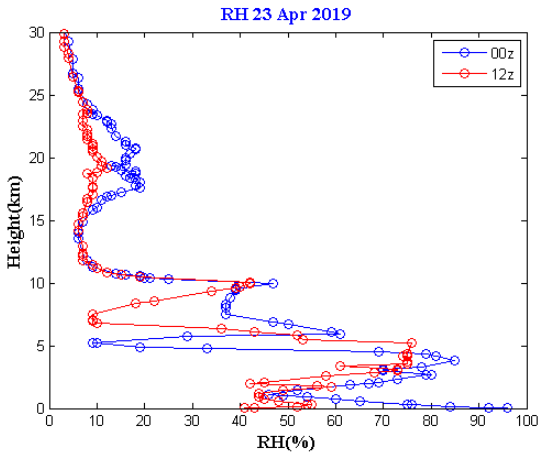
RH 23 Apr 2019
00z
12z
Height(km)
RH(%)

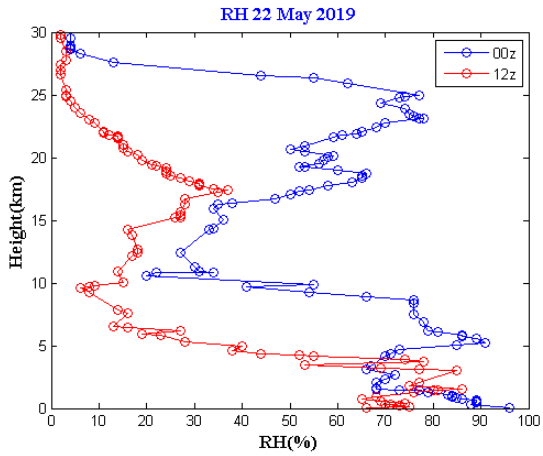
RH 22 May 2019
00z
12z
Height(km)
RH(%)

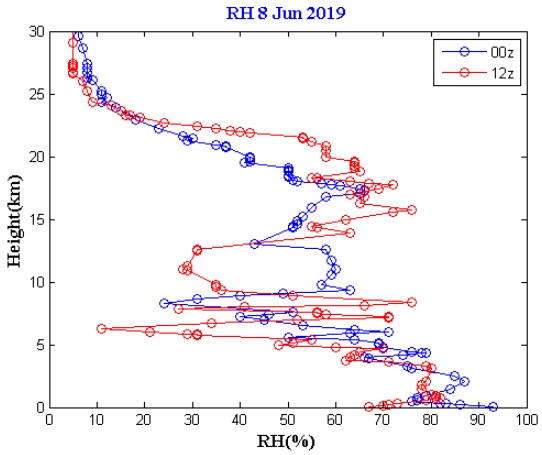
RH 8 Jun 2019
00z
12z
Height(km)
RH(%)

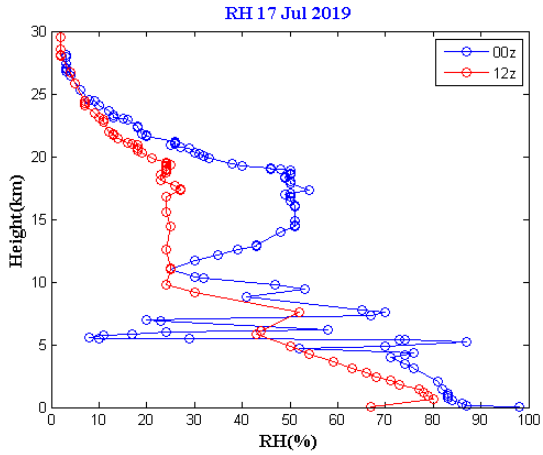
RH 17 Jul 2019
00z
12z
Height(km)
RH(%)

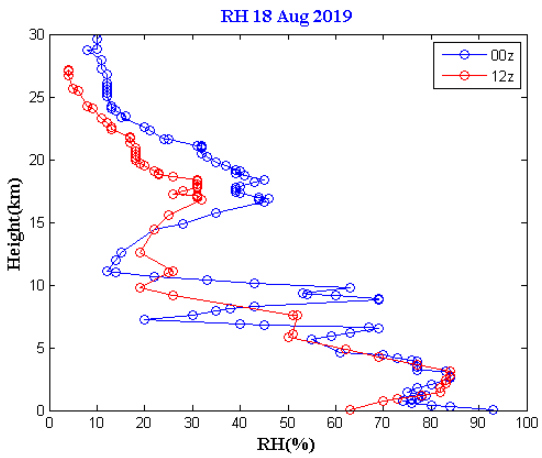
RH 18 Aug 2019
00z
12z
Height(km)
RH(%)

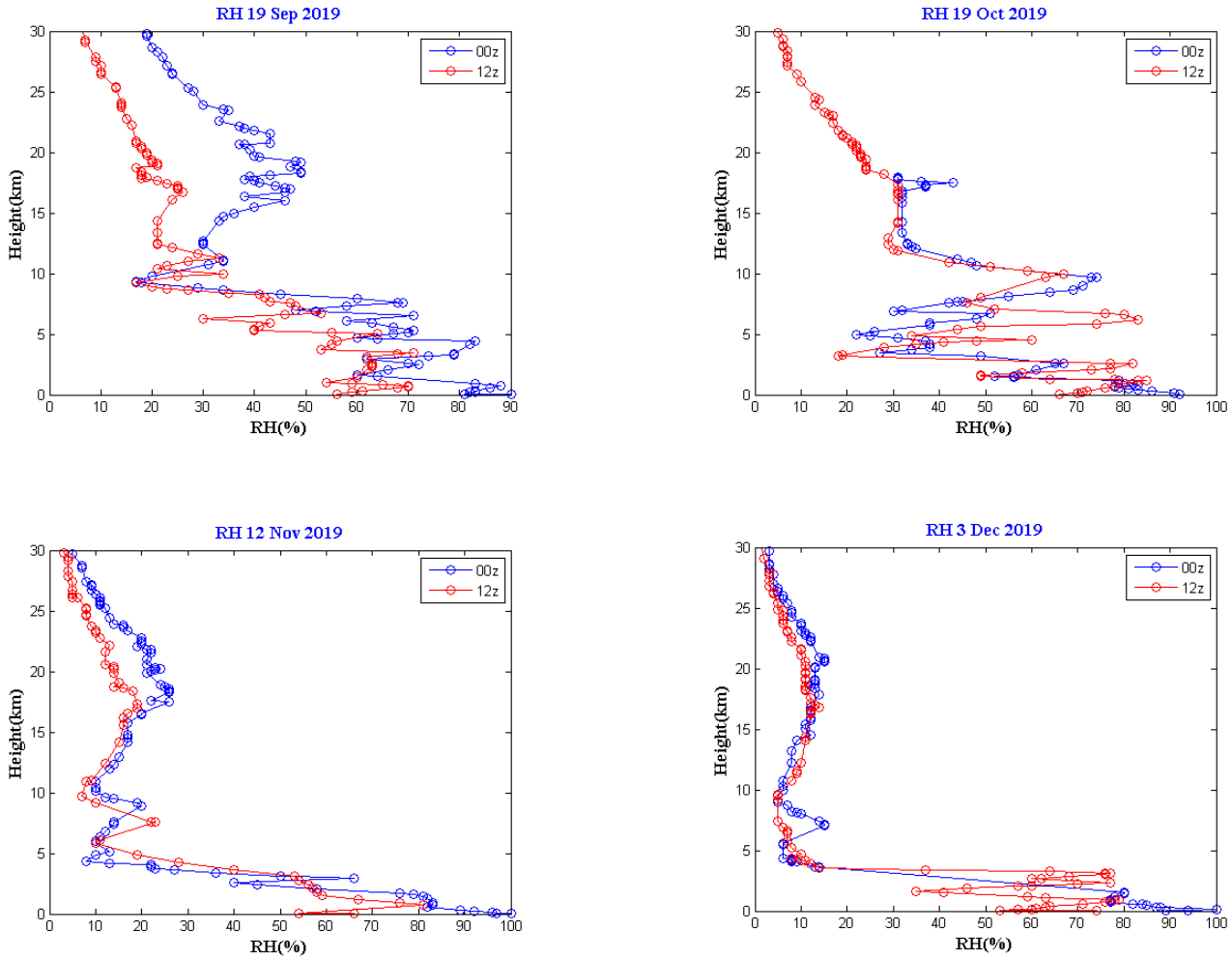

Figure 4.2: Vertical profiles of relative humidity at 00z and 12z for the cases under consideration.

Above the tropospheric height C_n^2 profiles for both the hours (00z and 12z) follow almost the same pattern as seen from the selected cases. It may be due to the fact that the moisture content at higher altitudes is nearly independent of the surface processes. Therefore, hourly variation of the upper level parameters on daily scale is less significant. In the upper tropospheric height, below 10 km, inversion peaks in the log (C_n^2) profiles can be seen for both the morning and afternoon hours of all the cases under consideration. Those peaks may be attributed to the share induced turbulence which can be explained through the hypothesis that turbulence is closely associated with the high wind speed components of the atmosphere. It is a well-known fact that, turbulence occurrence is very likely when the Richardson's number (R_i) is less than 0.25.

$$R_i = \frac{N^2}{S^2} < 0.25$$

Where N is buoyant stability and S is wind share parameters.

For a turbulent flow, S must exceed N value. In the free atmosphere where N is almost constant, Richardson magnitude is solely decided by the wind shear values. Therefore, under the above situations, turbulence is generated by strong shear conditions. Wind speed plots for the above cases are presented in figure 4.3. High wind speed components (>30 m/s) can be seen at upper tropospheric levels from November to May. From June onwards, the wind speed falls below 20 m/s up to October. The high wind shear during the winter and pre-monsoon months contributes to the sharp rise in atmospheric turbulence below tropopause.

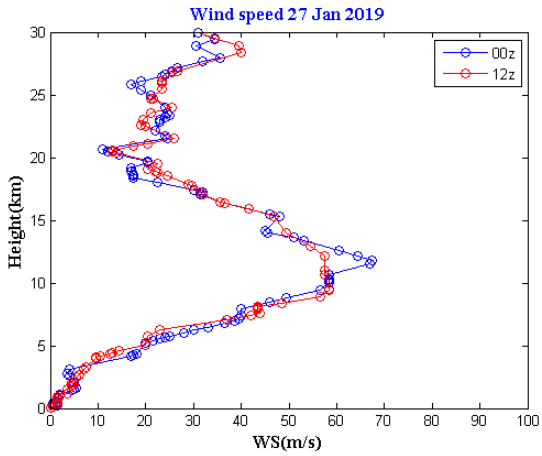

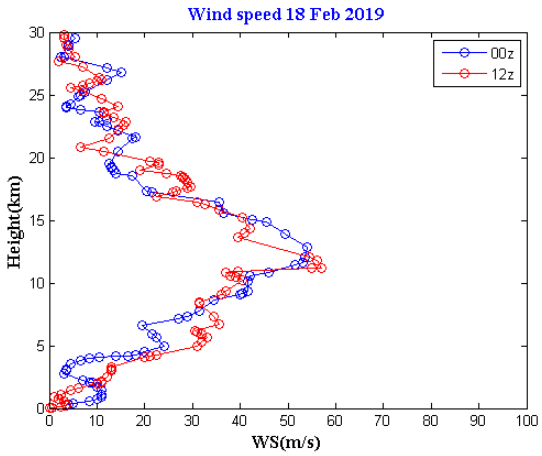

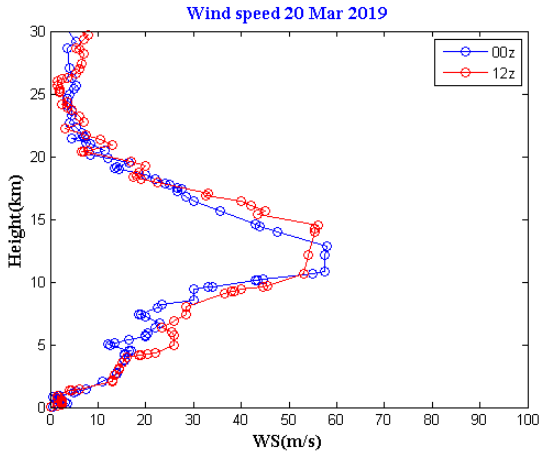

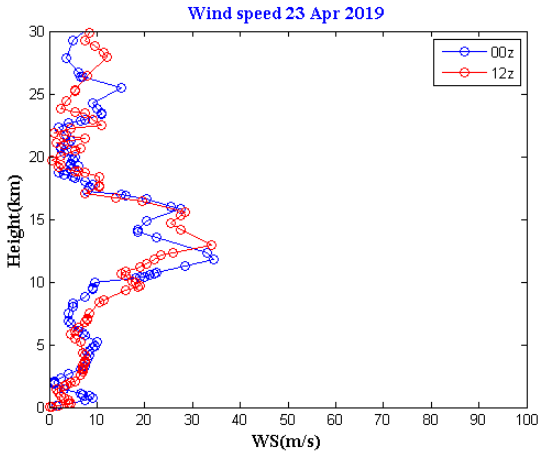

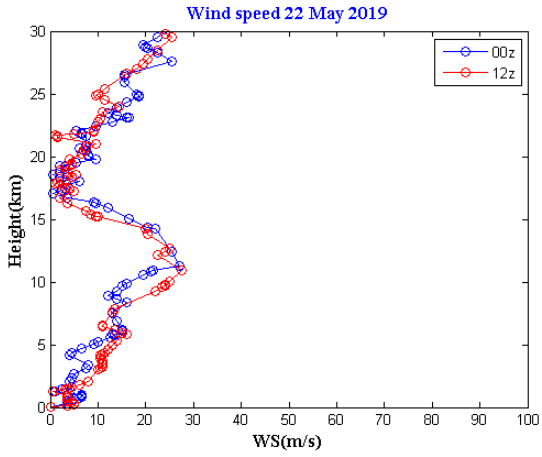

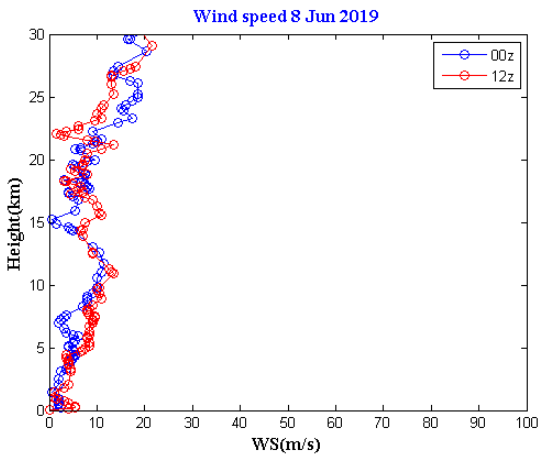

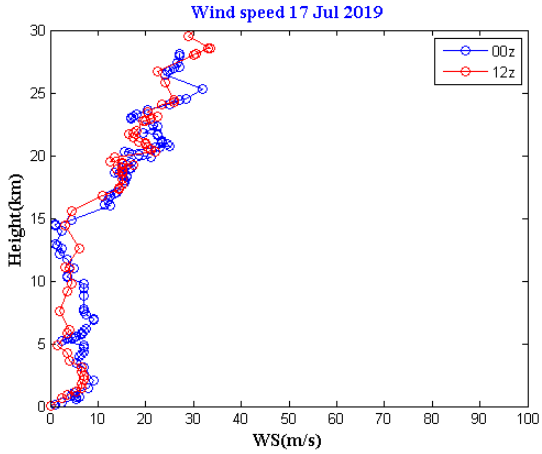
Wind speed 17 Jul 2019
00z
12z
Height(km)
WS(m/s)

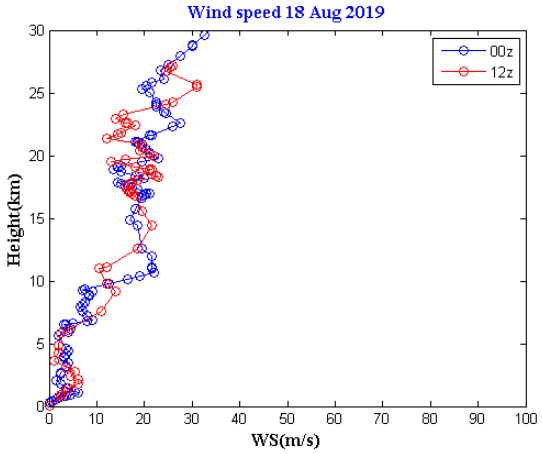
Wind speed 18 Aug 2019
00z
12z
Height(km)
WS(m/s)

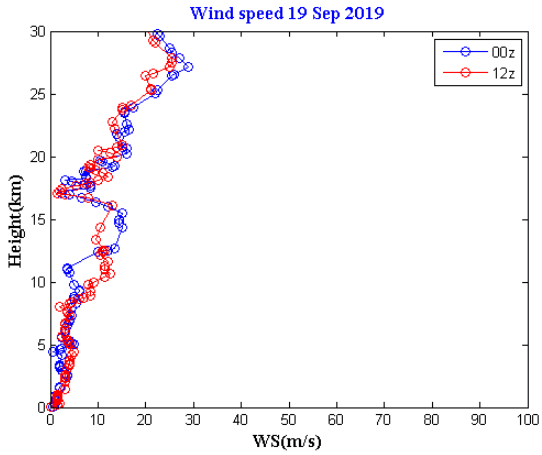
Wind speed 19 Sep 2019
00z
12z
Height(km)
WS(m/s)

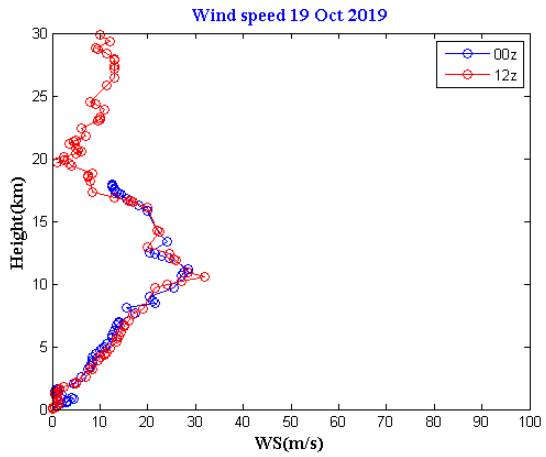
Wind speed 19 Oct 2019
00z
12z
Height(km)
WS(m/s)

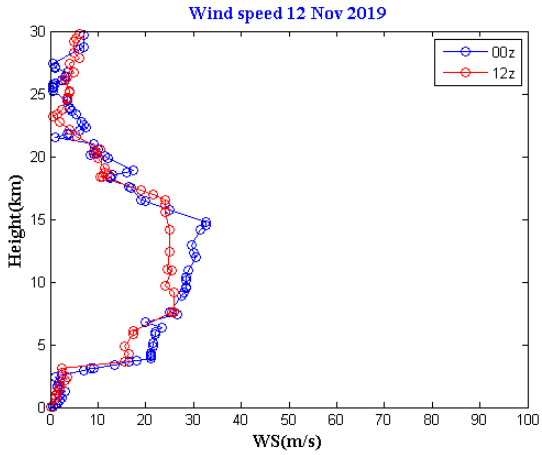
Wind speed 12 Nov 2019
00z
12z
Height(km)
WS(m/s)

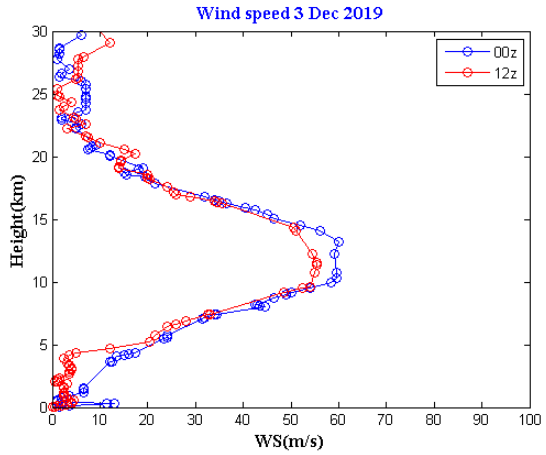
Wind speed 3 Dec 2019
00z
12z
Height(km)
WS(m/s)

Figure 4.3: Vertical profiles of wind speed(m/s) at 00z and 12z for the cases under consideration.

5. Conclusion

Morning and evening time C_n^2 characteristics over Guwahati are studied for 12 random days of 2019. Structure constant with higher magnitudes, at lower atmospheric heights are observed during both in the morning as well as in the evening hours as compared to the higher altitudes. Presence of the high moisture and temperature gradients at lower atmospheric levels may be the primary factor for high potential refractive index gradient and also higher C_n^2 magnitude at lower levels. During the monsoon months, transport of moisture by the seasonal wind from the Bay of Bengal also contributed to the enhancement of C_n^2 magnitude at higher level over the study region. In other season, at higher altitude, moisture gradient low and hence its contribution towards turbulence intensity is also not very significant. Noticeable turbulence inversion peaks at middle tropospheric heights are observed in all the cases. Those peaks may be attributed to the sharp wind shear gradients at those altitudes, which need further detailed investigation.

CrediT author contribution statement

Dhrubajyoti Choudhury: Conceptualisation, Methodology, Investigation, Formal Analysis, Visualisation, Writing-original Draft. **Dhanjit Medhi:** Investigation, Formal Analysis, Visualisation, Writing-original Draft. **Dhiman Barua:** Investigation, Formal Analysis, Visualisation , Writing-original Draft.

Declaration of competing interest:

The authors declare that they have no competing interests with respect to the research, authorship, and/or publication of this article.

Funding:

This work was not supported by any agency.

Availability of data :

The data generated and analysed during the present study are available from the corresponding author upon reasonable request.

Acknowledgement:

The authors would like to offer their sincere thanks to Dr. Hirakjyoti Goswami for some meaningful discussions and valuable suggestions. Authors would also like to thank the University of Wyoming for providing the opportunity of utilizing the Radio sonde data regarding various atmospheric parameter. Last but not least, the authors thank Department of Physics, Gauhati University for providing lab facility.

References

1. Martini E, Freni A, Cuccoli F, Facheris L (2017) Derivation of clear-air turbulence parameters from high-resolution radiosonde data. JTECH 34(2):277-293. https://doi.org/10.1175/JTECH-D-16-0046.1
2. Cherubini T, Businger S.(2013) Another look at the refractive index structure function. JAMC 52(2):498-506. https://doi.org/10.1175/JAMC-D-11-0263.1
3. Rambabu, S., et al.(2013) Climatological Study of Turbulence Structure Constant over Two Tropical Stations, Mumbai and Guwahati in India.Current Science, vol. 104:944–50. JSTOR, http://www.jstor.org/stable/24092108.
4. Bean BR, Horn JD (1959) Radio-refractive-index climate near the ground. J. Res. Natl. Bur. Stand.63:259-271.
5. Nath D, Venkat Ratnam M, Patra AK, Krishna Murthy BV, Bhaskar Rao SV (2010) Turbulence characteristics over tropical station Gadanki (13.5 N, 79.2 E) estimated using high-resolution GPS radiosonde data. J. Geophys. Res 115(D7). https://doi.org/10.1029/2009JD012347
6. Gang S, Ning-Quan W, Li-Ming X, Yi W.(2012) Profile and character of atmospheric structure constant of refractive index Cn2. AOSL 5(3):270-272.https://doi.org/10.1080/16742834.2012.11446990
7. Wilson R, Pitois C, Podglajen A, Hertzog A, Corcos M, Plougonven R(2023). Detection of turbulence occurrences from temperature, pressure, and position measurements under superpressure balloons. Atmospheric Measurement Techniques.20:311-330. https://doi.org/10.5194/amt-16-311-2023
8. Muhsin M, Sunilkumar SV, Ratnam MV, Parameswaran K, Mohankumar K, Mahadevan S, Murugadass K, Muraleedharan PM, Kumar BS, Nagendra N, Emmanuel M.(2020) Contrasting features of tropospheric turbulence over the Indian peninsula. JASTP 197:105179. https://doi.org/10.1016/j.jastp.2019.105179
9. Qing C, Wu X, Li X, Tian Q, Liu D, Rao R, Zhu W (2017) Simulating the Refractive Index Structure Constant(C_n^2) in the Surface Layer at Antarctica with a Mesoscale Model. AJ.155(1):37. https://doi.org/10.3847/1538-3881/aa9e8f
10. Ansari MI, Kundu SK, Saikrishnan KC, Madan R (2013) Measurement and analysis of refractive index structure constant Cn2 profile over Delhi on diurnal and seasonal basis. Mausam 64(2):363-370. https://doi.org/10.54302/mausam.v64i2.693
11. Frederickson PA, Davidson KL, Zeisse CR, Bendall CS (2000) Estimating the refractive index structure parameter (C_n^2) over the ocean using bulk methods. JAMC 39(10):1770-1783. https://doi.org/10.1175/1520-0450-39.10.1770
12. Shikhovtsev AY, Kovadlo PG, Kopylov EA, Ibrahimov MA, Ehgamberdiev SA, Tillayev YA (2021). Energy spectra of atmospheric turbulence for calculating C_n^2 parameter. I. Maidanak and Suffa observatories in Uzbekistan. atm12(12):1614. https://doi.org/10.3390/atmos12121614
13. Wu S, Wu X, Su C, Yang Q, Xu J, Luo T, Huang C, Qing C (2021) Reliable model to estimate the profile of the refractive index structure parameter (C n 2) and integrated astroclimatic parameters in the atmosphere. Opt. Express.29(8):12454-12470. https://doi.org/10.1364/OE.419823
14. Frehlich R, Sharman R (2004). Estimates of turbulence from numerical weather prediction model output with applications to turbulence diagnosis and data assimilation. Mon. Weather Rev 132(10):2308-2324. https://doi.org/10.1175/1520-0493(2004)132%3C2308:EOTFNW%3E2.0.CO;2

15. Cuevas O, Marin JC, Blazquez J, Meyer C (2024). Combining C_n^2 models to forecast the optical turbulence at Paranal. MNRAS.529(3):2208-2219. https://doi.org/10.1093/mnras/stae630
16. Bianco L, Wilczak JM(2002) Convective boundary layer depth: Improved measurement by Doppler radar wind profiler using fuzzy logic methods. JTECH 19(11):1745-1758. https://doi.org/10.1175/1520-0426(2002)019%3C1745:CBLDIM%3E2.0.CO;2
17. Saïd F, Campistron B, Di Girolamo P (2018). High-resolution humidity profiles retrieved from wind profiler radar measurements. Atmospheric Measurement Techniques. 11(3):1669-1688. https://doi.org/10.5194/amt-11-1669-2018